LIMNOLOGY and OCEANOGRAPHY

ASLO

Limnol. Oceanogr. 9999, 2021, 1–17

doi: 10.1002/lno.11789

Metabolic regime shifts and ecosystem state changes are decoupled in a large river

Jacob S. Diamond [1,2*] **Florentina Moatar** [1] **Matthew J. Cohen,** [3] **Alain Poirel,** [4] **Cécile Martinet,** [4] **Anthony Maire** [5] **Gilles Pinay** [6]

[1]INRAE, RiverLy, Centre de Lyon-Grenoble Auvergne-Rhône-Alpes, Villeurbanne, France
[2]GéoHydrosytèmes COntinentaux, Université de Tours, Tours, France
[3]School of Forest Resources and Conservation, University of Florida, Gainesville, Florida
[4]Division Technique Générale, Électricité de France, Grenoble, France
[5]Électricité de France—Laboratoire National d'Hydraulique et Environnement, Chatou, France
[6]Environnement, Ville & Société (EVS UMR5600), Centre National de la Recherche Scientifique (CNRS), Lyon, France

Abstract

Aquatic ecosystem recovery from anthropogenic degradation can be hampered by internal feedbacks that stabilize undesirable states. The challenges of managing and predicting alternative states in lakes are well known, but state shifts in rivers and their attendant effects on ecosystem function remain understudied despite strong recent evidence that such shifts can and do occur. Using three decades of measurements of key state variables such as turbidity, nutrient concentrations, *Corbicula fluminea* clam densities, and chlorophyll *a*, including hourly dissolved oxygen, we investigated a sudden shift from phytoplankton to macrophyte dominance in the middle Loire River (France), and its associated effects on the rivers metabolic regime. We show, instead, that despite large and synchronous shifts across all state variables, changes in gross primary production and ecosystem respiration were modest (25% and 14% declines, respectively) and that these shifts lagged the ecosystem state changes by a decade or more. The shift to a macrophyte-dominated state reduced the sensitivity of primary production to abiotic drivers, altered element cycling efficiency, flipped the net carbon balance from positive to negative, and, crucially, weakened the temporal coupling between production and respiration. This weakened coupling, detected using Granger causality, increased the temporal autocorrelation of net ecosystem production, yielding a robust early warning indicator of both state- and metabolic-shifts that may provide valuable guidance for river restoration.

Abrupt shifts in aquatic ecosystem state, generally between starkly contrasting autotrophic communities (Scheffer and Jeppesen 2007; de Tezanos Pinto and O'Farrell 2014), are linked to changes in the internal feedbacks that define system resilience. These state shifts can occur in response to enrichment of a growth-limiting nutrient (Jarvie et al. 2013), altered food-web structure (Carpenter et al. 2011), and changing disturbance regimes (Heffernan 2008). Anticipating these state shifts, and recovering from them, is a major practical and theoretical challenge (European Environmental Commission 1991; Biggs et al. 2009), particularly given the long lags between remedial actions and ecosystem responses that can occur when undesirable states are themselves resilient. Understanding and predicting the trajectory of state shifts in managed aquatic ecosystems is crucial for maintaining stakeholder engagement, and accurately attributing observed changes to specific remedial actions.

Aquatic ecosystem state shifts are well-documented in shallow lakes (Scheffer and Jeppesen 2007) and estuaries (Cohen et al. 1984), but are less common in rivers (Jarvie et al. 2013; Capon et al. 2015). The high nutrient availability due to constant upstream replenishment (King et al. 2014; Covino et al. 2018), short hydrochemical residence times, and intrinsic hydrological disturbance regimes of most rivers suggest that the internal stabilizing feedbacks necessary to induce resilient states are, in relation to lakes, comparatively weak or nonexistent (Hilton et al. 2006; Hilt 2015). However, evidence suggests that some large rivers do exhibit state shifts analogous to those of shallow lakes. A state shift returning from eutrophic, phytoplankton dominance to oligotrophic, macrophyte dominance (i.e., re-oligotrophication) has been attributed to reduced phosphorus loading (Hilt et al. 2011; Ibáñez et al. 2012; Ibáñez and Peñuelas 2019) and top-down control

*Correspondence: jacob.diamond@inrae.fr

Additional Supporting Information may be found in the online version of this article.

from invasive *Corbicula fluminea* clams (Minaudo et al. 2020). Still, the causes and time scales of these changes—which help focus remedial actions, calibrate public expectations, and set meaningful interim management targets—remain poorly constrained.

The amplification of planktonic biomass production under eutrophic conditions (Smith et al. 1999) suggests a coherence between ecosystem state and ecosystem metabolic regime. Ecosystem metabolism, which describes the magnitude of gross primary production (GPP) and ecosystem respiration (ER), has a rich legacy of measurement in lotic systems (Odum 1956) and is a foundational part of stream ecosystem theory (Vannote et al. 1980). Yet, despite broad understanding on environmental controls (Mulholland et al. 2001) and more recently on spatiotemporal regimes (Koenig et al. 2019; Savoy et al. 2019), little is known regarding how metabolism and its sensitivity to environmental drivers change under contrasting autotrophic communities (e.g., those dominated by rooted macrophytes vs. those dominated by phytoplankton). Indeed, the magnitude and timing of the coupling between ecosystem state shifts and metabolic functions has only been described recently in lakes (Hilt et al. 2017), and remains entirely unknown in rivers (Williamson et al. 2008; Palmer and Ruhi 2019). Recent growth in long time series of dissolved oxygen (DO; Bernhardt et al. 2018) and model estimation of GPP and ER in flowing water systems (Appling et al. 2018) enable new insights into metabolic variation and controls across time scales. These modern tools have only recently been used to explore the functional consequences of changing river management (Arroita et al. 2019), but have yet to be used to evaluate the character of ecosystem state shifts.

Large rivers provide valuable ecosystem functions, including substantial biotic processing of macronutrients (Seitzinger et al. 2002; Cohen et al. 2013) and (Cole et al. 2007; Escoffier et al. 2018). Because these biogeochemical functions derive from a river's metabolic activity, a putative regime shift in metabolism will likely induce shifts in biogeochemical cycling and process rates, but the mode, timing, and magnitude of these shifts are unknown. For example, the degree of coupling between GPP and ER—i.e., how rapidly C produced by autotrophs is consumed (Hall and Beaulieu 2013; Hotchkiss and Hall 2015)—is a function of the quality and distribution of internal organic matter stocks, with planktonic algae more readily consumed (Lair and Reyes-Marchant 1997) than macrophtyes (del Giorgio and Williams 2005). Moreover, lower C storage in a planktonic state compared to a macrophyte state (because plankton are readily exported from the system and lack roots to stabilize sediment organic matter) may reduce the temporal stability of C stocks available for consumption. Critically, changes to GPP-ER coupling and C storage under different autotrophic communities may lead to shifts in mode, magnitude, and temporal patterns of net ecosystem productivity (NEP = GPP + ER; where ER is negative in sign).

In aquatic ecosystems, regime shifts from oligotrophic to eutrophic conditions are presaged by "early warning signals" (Scheffer et al. 2015), which can aid managers seeking to anticipate critical transitions or even prevent them from taking place (Biggs et al. 2009). These early warning signals (Gsell et al. 2016) generally result from declining ecosystem state resilience and are theoretically and empirically manifest in time series properties of state variables like phytoplankton biomass, or phosphorus concentration. Specifically, the early warning signals include increases in temporal autocorrelation (Batt et al. 2013), variance (Carpenter and Brock 2006), and skewness (Guttal and Jayaprakash 2008). However, nearly all early warning signal applications in aquatic ecosystems have been used to detect the onset of phytoplankton dominance, and have almost exclusively employed state variables, as opposed to process rate time series (though see Batt et al. 2013). As such, open questions remain regarding the detection of regime shifts in the opposite direction (i.e., re-oligotrophication), and applicability of process rate time series, like ecosystem metabolism, to predict state transitions.

We focus here on the changes that shifts in river ecosystem state have on function in the Loire River in France, a minimally disturbed large river with detailed ecological and hydrochemical monitoring, including 25 yr of hourly DO measurements. The middle Loire River recently underwent a dramatic re-oligotrophication shift (Minaudo et al. 2015, 2020), manifested as sudden declining concentrations of phosphorus, algal pigments, and turbidity during the summer growing season. We first investigated how and when these ecosystem state changes influenced the river metabolic regime. We further used these rich datasets to evaluate early warning indicators of shifts in ecosystem state (i.e., phytoplankton to macrophyte dominance) and metabolic regimes (Scheffer et al. 2015). Specifically, we tested four linked hypotheses. First, we hypothesized that the observed dramatic decreases in phytoplankton biomass in the middle Loire River are indeed a regime shift to an alternative stable state. This leads to the prediction that state changes are discrete, synchronous, and durable. Second, we hypothesized that the river metabolic regime shifted synchronously with ecosystem state changes in the Loire River. This leads to the prediction that change-points in both state and process time series occur at the same time. Third, we hypothesized that any metabolic regime shift would be accompanied by changes to linked biogeochemical processes. Specifically, we predicted declining sensitivity of primary production to abiotic controls (e.g., flow, light, temperature), decreased elemental (i.e., C and N) removal efficiency, and a shift in the balance of GPP and ER toward heterotrophy in association with decreased temporal coupling between these metabolic processes prompted by the switch to macrophyte dominance. Finally, we hypothesized that both ecosystem state and metabolic regime shifts can be predicted with early warning indicators derived from both

ecosystem state and process rates. Moreover, given the expectation that the temporal coupling of GPP and ER declines in the macrophyte state, we predicted that time series of their metabolic balance (i.e., NEP) will yield insights about incipient shifts.

Methods

Site description

The 10-km study reach is located on the upper section of the middle Loire, France, between Saint-Satur (47.3°N 2.9°E) and Dampierre-en-Burly (47.4°N; 2.3°E). In this reach, the Loire is an 8th-order river, with a catchment area of 35,500 km^2, a mean width of 250 m and a mean depth of 1 m during summer base flow. Dampierre-en-Burly is at an altitude of 123 m a.s.l., 110 km downstream from the confluence with the Allier River and 550 km from the Loire's source. The region is dominated by calcareous bedrock and sedimentary alluvial valleys (Baratelli et al. 2016). The middle Loire has a shallow bed slope (0.44 m km^{-1}) and wide, braided channels flowing over calcareous tables and around vegetated islands that reduce flow velocity and allow for warming (Moatar and Gailhard 2006).

Intensive agriculture (70% of land cover) and human development (40% of the watershed population) in the middle Loire River likely led to dramatic nutrient enrichment, which was particularly evident starting in the early 1980s, and lasted for approximately 25 yr (Moatar and Meybeck 2005). During this time, the Loire River also experienced trends of rising water temperature, reduced flow (Moatar and Gailhard 2006), rapid expansion of invasive *Corbicula fluminea* filter feeders (Floury et al. 2013). Then, in the past 15 yr, the river has exhibited dramatic decreases in phosphorus (Minaudo et al. 2015), suspended organic matter (Minaudo et al. 2016), and planktonic biomass (Minaudo et al. 2020).

Data acquisition and processing

We obtained hourly DO and water temperature data (Fig. S1) from 1993 to 2018 from a regulatory dataset maintained and collected by Électricité de France (EDF) upstream of the Dampierre nuclear power plant (47.4°N; 2.3°E). Measurements are made on pumped water from the middle of the river. While the data were quality-controlled for sensor drift and outlier removal by the agency using methods developed by Moatar et al. (2001), we conducted additional control using low-pass data filtering and outlier removal based on visual inspection.

We used Kalman interpolation (with R package *imputeTS*, Moritz and Bartz-Beielstein 2017) to fill data gaps in DO and water temperature time series where gaps were less than 1 d (days with gaps were less than 1% of all data); gaps longer than 1 d were assigned NA values and omitted from further analysis. We estimated DO saturation concentration (i.e., DO concentration at equilibrium with atmospheric oxygen) as a function of water temperature (°C), and we estimated water depth (m) from a depth-discharge rating curve established for the study site. Short-wave radiation (W m^{-2}) data were obtained from a nearby meteorological station and converted to photosynthetically active radiation (PAR, 400–700 nm, μmol m^{-2} s^{-1}). We gap-filled periods without measured PAR using estimates based on latitude and longitude (Fig. S1).

Available long-term water quality characteristics included water column concentrations of nitrate (NO_3–N), phosphate (PO_4–P), biochemical oxygen demand (BOD_5), dissolved organic carbon (DOC), total suspended solids (TSS), and chlorophyll *a* (http://www.naiades.eaufrance.fr/, Diamond 2021; Table S1). Most were recorded at Jargeau (47.9°N; 2.1°E) on a monthly basis from 1980 to 2018 by the Loire-Bretagne Basin Water Agency. To increase sampling frequency and time series length, we supplemented these data with measurements from a station 20 km downstream at Orléans (47.9°N, 1.9°E), which we justify given that water chemistry (particularly chlorophyll *a*) was similar between the two stations on days with coincident measurements (e.g., $\beta = 0.84$, $R^2 = 0.74$, $p < 0.001$ for chlorophyll *a*).

We obtained summertime estimates (1997–2018) of macrophyte areal cover from the nearby St. Mesmin Nature Reserve (47.87°N, 1.82°E), where species-level cover was measured at 24 transects (60 m long by 5 m wide) over a 7.5 km reach (overall area sampled = 7200 m^2). We calculated areal macrophyte cover percentages by dividing their measured area by the total sampling area.

We also obtained summertime *Corbicula fluminea* densities from EDF (1991–2018), which were quantified with the Surber technique. We estimated clam filtration rates (m^3 d^{-1}) in the river reach with literature values for individual clams (McDowell and Byers 2019) scaled to measured densities (individuals m^{-2}) and estimated reach benthic area (250 m wide $\times$ 10 000 m long). To quantify the relative importance of clam filtration rates, we divided the hydraulic residence time of water within the 10-km reach (reach volume/median daily summer discharge, [d]) by the time needed for clams to filter the water within the reach (reach volume/scaled filtration rate, [d]) (McDowell and Byers 2019). This unitless "turnover ratio" estimates the number of reach volumes filtered by clams at baseflow; when clams filter as rapidly as discharge (i.e., ratio values of 1) the clams filter all of the incoming water within the reach.

For all analyses, we focus on the growing season (April–October) for two reasons: (1) the time frame includes periods of maximal biological activity; and (2) the growing season minimizes confounding effects of predictable disturbance events (e.g., floods, freezing) common in winter. As such, summer includes biotically driven signal-to-noise ratios that are greatest, providing the optimal conditions for testing hypotheses presented here. Indeed, as our metabolic measurements ultimately show, GPP is effectively nil (as are 40% of ER estimates) outside of the growing season, limiting its

inferential utility during that time, and justifying our emphasis on analyses of summer measurements only.

Metabolism calculations

We used a single-station open channel method to estimate stream metabolism (Odum 1956). We estimated daily fluxes for GPP (g O_2 m^{-2} d^{-1}), ER (g O_2 m^{-2} d^{-1}), and reaeration (k_{600} [d^{-1}]) using inverse fitting of DO dynamics with a state space approach (i.e., including process and observation error) and Bayesian inference with Markov chain Monte Carlo sampling (Appling et al. 2018). To constrain k_{600}, we pooled its estimates based on discharge, corresponding to the *b_Kb_oipi_tr_plrckm.stan* model in the *streamMetabolizer* R package (version 0.10.9) (Appling et al. 2018). The hyperprior, i.e., the prior distribution of the mean of k_{600} for all days, was lognormally distributed—Lognormal(1.1, 0.1)—which was based on O'Connor and Dobbins equations (O'Connor and Dobbins 1958) and floating dome measurements (G. Abril, unpublished, Table S2). Priors for daily GPP and ER were normally distributed—N(8, 6) and N(−7.1, 7.1), respectively—where GPP was based on literature ranges from prior unpublished investigations and ER was based on developer recommendations. Four Markov chains were run in parallel on four cores, with 1000 warmup steps and 500 saved steps on each chain. Additional information on metabolism calculations is provided in the Supporting Information (Figs. S1–S3).

Regime shift and stable state detection

We first evaluated regime shifts in ecosystem state (i.e., TSS, chlorophyll *a*, BOD_5, PO_4–P, NO_3–N, *Corbicula fluminea* density, and macrophyte cover) and metabolism (i.e., GPP and ER) with a statistical change point analysis, which identified the point in each time series where the mean and variance shifted. The presence of a change point indicates a likely regime shift in the time series. Where change points are detected at similar times (i.e., within estimated uncertainty bounds) among different variable time series, we interpret the implied regime shifts as coincident; coincidence among variables is one indicator that the detected change points are associated with an ecosystem state shift.

Change points in our time series were detected using generalized, hierarchical linear models with Bayesian inference (R package *mcp*, Lindeløv 2020). We fit generalized linear models to our time series and prescribed the inclusion of discrete changes in mean and variance. We then provided uniformly distributed priors of change points based on visually obvious shifts in time series, but ensured they were 4 yr wide to minimize confirmation bias (e.g., if the time series exhibit a clear change point in July 2005, our prior distribution as uniform between July 2003 and July 2007). We evaluated convergence for the change point, and the means and variances before and after the change point ($n_{\text{param}} = 5$) using the Gelman-Rubin R diagnostic, ensuring its value was <1.01. The output includes a best estimate of the change point and its 95% credible interval (i.e., Bayesian equivalent to confidence intervals). We calculated growing season mean and variance before and after the change point for each variable to compare the relative magnitude of change.

To assess the plausibility of stable, resilient alternative riverine stable states similar to those observed in shallow lakes, we created phase space plots relating known drivers (PO_4–P, *Corbicula fluminea* density) and response variables (chlorophyll *a* and TSS). We also did the same for metabolism (GPP vs. chlorophyll *a* and PO_4–P) to assess if metabolic regimes exhibited stable regime behavior. Each phase space plot shows the interannual trajectory of representative summer values for each variable with presumed drivers on the *x*-axis and response variables on the *y*-axis. Where a rapid shift between alternative states (or metabolic regimes) occurs driven by strong internal feedbacks, the phase-space plots exhibit an "S" shaped pattern (e.g., Scheffer et al. 2001) where both low and high values of a response variable are possible at the same value of the driver variable. Strong clustering of points at either end of the "S" curve indicate stable regions of the ecosystem state space. If shifts are not regulated by internal feedbacks that confer stability, or these feedbacks are weak, these plots will exhibit smooth, monotonic behavior; sudden transitions between strongly contrasting phases indicate the presence of internal feedbacks that lead to resilient ecosystem states.

Temporal shifts in ecosystem processes

We quantified four facets of ecosystem changes following regime shifts in both ecosystem state variables and metabolic function. First, we evaluated the changing abiotic controls on GPP, following our prediction that the macrophyte state is less sensitive to variation in light, temperature and discharge due to more temporally stable biomass stocks. Second, we evaluated changes in biological removal efficiencies for C and N, following our prediction that these will decrease with a switch to macrophyte dominance and the acquisition of nutrients from the sediments. Third, we evaluated changes in reach-scale C balance between GPP and ER following our prediction of increased persistence of biomass stocks under macrophytes. Finally, we evaluated the temporal coupling of GPP and ER following our prediction that it would be reduced with more stable biomass stocks under macrophyte-dominance.

Changing abiotic controls on GPP

Prior to evaluating how regime change altered abiotic control of GPP, we first determined the primary influences on GPP broadly across the time series with multiple linear regression. To do this, we used a best subsets approach with an exhaustive search algorithm (R package *leaps*, Lumley 2020) to compare growing season GPP against hypothesized drivers using measured physicochemical variables on days when all variables were measured coincidentally ($n = 181$). We centered and scaled variables so that model coefficient magnitudes would be comparable. We considered daily discharge, median

daily light, median daily water temperature, and grab samples of DOC, TSS, NO_3–N, PO_4–P, and chlorophyll *a* as potential drivers of GPP. After ensuring residuals were normally distributed and homoscedastic, we compared models with adjusted R^2, Mallow's Cp statistic, BIC, and the PRESS statistic.

To specifically evaluate changing strength in environmental drivers of GPP under changing regimes in the Loire River, we conducted a multiple linear regression. We used the dominant environmental drivers identified by previous regression analysis as our predictor variables with regime as an interaction term. Metabolism measurements prior to the change point were considered indicative of the phytoplankton metabolic regime, and measurements after the change point were indicative of the macrophyte metabolic regime. Prior to our analysis, we centered and scaled the data so that coefficients between would be comparable. To avoid residual autocorrelation, we randomly sampled the dataset to yield 200 points in each regime. Where the interaction term was significant, indicating change in the nature of control, we further compared the magnitude of regression coefficients for the environmental drivers within each regime type to assess their changing strength between regimes.

Changing biological removal efficiencies

We quantified reach-scale nutrient removal efficiency using the Damköhler number (Da), a unitless ratio relating reactivity to transport (Da = removal rate / transport rate). Da values below one indicate that transport through the system dominates and removal is rate-limited (e.g., by biotic assimilation capacity), whereas Da values greater than one indicate that reactivity in the system dominates and removal is supply-limited. We calculated Da for both C and N as the ratio of biological removal (in g $month^{-1}$) to the river loading (g $month^{-1}$), where removal and loading were obtained from monthly average values for August. We chose August because it is the most stable baseflow month (99 ± 56 m^3 s^{-1}; mean ± SD), allowing for (1) consistent hydraulic travel times across years and therefore comparable reach lengths and benthic surfaces to scale areal removal rates, and (2) ideal conditions to isolate effects of biotic element removal.

We postulated that reach-scale mass removal for C was defined by ER, and for N was equal to autotrophic NO_3–N uptake (g NO_3–N m^{-2} $month^{-1}$). For both C and N biological load removal, we scaled areal fluxes (g m^{-2} $month^{-1}$) to the reach area, with the length estimated as the distance water travels over 1 d (~10 km in summer baseflow) and width based on average width over this travel distance (~250 m). We estimated autotrophic nitrate uptake from GPP (Heffernan and Cohen 2010) in C units and an assumed C:N stoichiometry for phytoplankton (8:1) and macrophytes (20:1) (Ventura et al. 2008). We made the simplifying assumption, based on clear evidence of ecosystem state shift from phytoplankton to macrophytes that all autotrophic nitrate uptake was attributed to phytoplankton prior to the state shift and was attributed to macrophytes after the state shift.

River loads were calculated by multiplying measured concentration and discharge. For C, we used total organic carbon (TOC) concentration (g m^{-3}) as the constituent of interest because it describes the potential organic matter pool for respiration. TOC was the sum of DOC and particulate organic carbon (POC), where POC was estimated from total pigments (chlorophyll *a* and pheophytin) using literature conversion values derived for this river (Minaudo et al. 2016). For N, we used total inorganic nitrogen (TIN) concentration as the constituent of interest because it describes the overall pool available to autotrophic assimilation. We calculated TIN as the sum of NO_3–N and ammonium ion concentrations (nitrite is less than detection for most sampling dates).

Decreased NEP and C balance

To determine the shifting balance between GPP and ER associated with state and metabolic regime shifts we evaluated the sign and magnitude of NEP integrated over the growing season for a representative river reach. Positive NEP implies net organic C accrual within the river reach ("net autotrophy"), while negative NEP implies net CO_2 efflux out of the river reach ("net heterotrophy"). A shift from autotrophy to heterotrophy constitutes a meaningful change in biological processing of C in the river. To emphasize the NEP effect on the C balance, we estimated longitudinal C efflux or accrual (Mg C km^{-1}) from the river reach by first converting daily NEP rates in units of g O_2 m^{-2} d^{-1} to commensurate C units, assuming molar respiratory and photosynthetic quotients of 1 (King et al. 2014). We then scaled average daily growing season value of NEP (g C m^{-2} d^{-1}) to the mean reach width (250 m) and the growing season length (180 d). This approach assumes rapid exchange of respired CO_2 with the atmosphere, and negligible transformation to other aqueous inorganic forms (e.g., bicarbonate) with downstream transport out of the reach.

Decoupling of temporal variation in GPP and ER

We quantified the coupling between GPP and ER using Granger causality, an approach broadly useful for detecting interactions between strongly coupled, or synchronized, variables in nonlinear systems (Sugihara et al. 2012). While river and stream GPP and ER are typically highly correlated on daily timescales, these correlations are not necessarily or entirely causal because GPP and ER have shared exogenous drivers (e.g., temperature). Granger causality was applied in an effort to parse the effect of GPP on ER—i.e., the effect of C fixed by photosynthesis in a given day on community respiration on that same day, or the day after. Granger causality tests whether past values (limited to a lag of 1 d in this case) of GPP are useful for predicting ER once the ER time series has been modeled with a vector autoregressive model. The null hypothesis, tested with a Wald test, is that past values of GPP do not predict ER values. That is, GPP and ER are temporally

decoupled. We grouped each metabolic time series by year and conducted the test for each year. We extracted Wald test *p*-values for each year, and interpret *p*-values >0.05, indicating a failure to reject the null hypothesis, implying that GPP and ER are poorly coupled. By complement, Wald test $p < 0.05$ imply significant coupling.

Early warning indicators of regime shifts

For each of the metabolic and state variable time series, we calculated right-aligned moving window estimates ("early warning indicators") of variance, skewness, and lag-1 autocorrelation coefficient (ar[1]) at each date. The temporal resolution was monthly for grab sample data, and daily for GPP, ER, NEP, and the minimum, maximum, and diel ranges for DO concentration. In this procedure, there are (at least) two critical choices that affect the subsequent output interpretation: window length and detrending procedure. Hence, we conducted a series of sensitivity analyses to identify an optimal window length for each time series, as is commonly recommended (Dakos et al. 2012). The goal of these sensitivity analyses is to balance estimate precision, which increases with larger window sizes, with the ability to capture dynamics in the time series, which improves with smaller window sizes (Carpenter et al. 2011). We varied the length of our moving window estimates from between 5% and 50% of each time series length to evaluate the influence of window size on results (Dakos et al. 2012). We further tested the sensitivity of the early warning indicators to two commonly applied detrending procedures: Gaussian detrending to remove seasonality, and first differencing (Dakos et al. 2012).

We quantified the temporal evolution of the various early warning indicators with the nonparametric Mann–Kendall trend test, which tests for monotonic trends leading up to a change point based on the Kendall τ rank correlation coefficient (Scheffer et al. 2015). A high Kendall τ prior to a regime shift indicates that a given variable functions well as an early warning indicator. For example, a high Kendall τ could arise from the standard deviation of chlorophyll *a* increasing consistently leading up to the regime shift (as predicted by theory, Carpenter and Brock 2006) suggesting it serves as a viable indicator for anticipating the regime shift. We assumed a Kendall τ magnitude of 0.5 (cf. Dakos et al. 2012) to be a cut-off value to identify a variable as significant early warning indicator.

A simple re-oligotrophication model

We developed a simple model of the re-oligotrophication process with the purpose of first demonstrating how GPP and ER decoupling occurs—and NEP changes sign—as the biomass storage properties of the ecosystem change. The model served a second purpose in assessing how this decoupling may induce early warning signals in the NEP time series signal. The model represents the links between biomass structure (i.e., planktonic or sessile) and biomass export (Fig. S4). Biomass, the only state in the model, is driven by five fluxes: inputs of (1) GPP and (2) allochthonous upstream imports, and outputs of (3) autotrophic respiration (AR), (4) heterotrophic respiration (HR), and (5) downstream export, or biomass flushing (Fig. S4). While the model employs six parameters that control these fluxes, the only free parameter that we considered was the export rate, corresponding to the proportion of biomass exported with flow. Values for other parameters were based on estimates for the middle Loire River, where AR was assumed to be 50% of GPP and HR was assumed to be 20% of biomass. Here, the essence of the putative regime shift is proposed to be captured in the differing propensity for export under the alternative stable states. Accordingly, model output should provide similar early warning behavior as observed empirically for proposed indicators.

We ran the model for 25 yr on a daily time step (to mirror our metabolism time series), allowing the daily export rate to slowly decline from a uniform distribution from 0.1 to 0.9 (unif[0.1, 0.9]), representing a phytoplankton environment where 10%–90% of biomass can be exported on a given day, to unif(0.1, 0.2), representing a macrophyte environment where only 10%–20% of biomass can be exported on a given day. While a more complex model that considered actual discharge variation is more realistic, we selected this simple model because it generated similar results.

We compared the model output dynamics to observed time series patterns (i.e., ar[1], standard deviation, and skewness) of the state variables considered for early warning indicators. Specifically, using the same decision criteria for analyzing the model time series (rolling window size, detrending) we investigated whether the model replicated the time series patterns observed in the empirical data spanning the regime shift from phytoplankton- to macrophyte-dominance.

Results

Evidence of stable regime shifts in ecosystem state, but not process

The middle reach of the Loire River exhibited a dramatic and approximately synchronous change point in nearly all river ecosystem state variables—including TSS, PO_4–P, BOD_5, and NO_3–N—between 2002 and 2003, with a commensurate shift in water column concentrations of chlorophyll *a* approximately 3 yr later (2005; Fig. 1a–e). These shifts were large (changes of −75% TSS, −75% PO_4–P, −60% BOD_5, −90% chlorophyll *a*; and +25% NO_3–N, Fig. 1a–e, right panels) and sudden, occurring within a narrow credible time span, especially for N, P and chlorophyll *a*. Notably, while PO_4–P concentrations had been declining slowly since the early 1990s (Fig. S5), the shift between 2002 and 2003 was far larger, and inverted the seasonal patterning to yield low summer concentrations. The TSS change point exhibited the widest credible intervals (approximately 7 yr), followed by BOD_5 (approximately 3 yr), whereas other state variables' uncertainties were constrained to approximately 1 yr. Submerged macrophyte

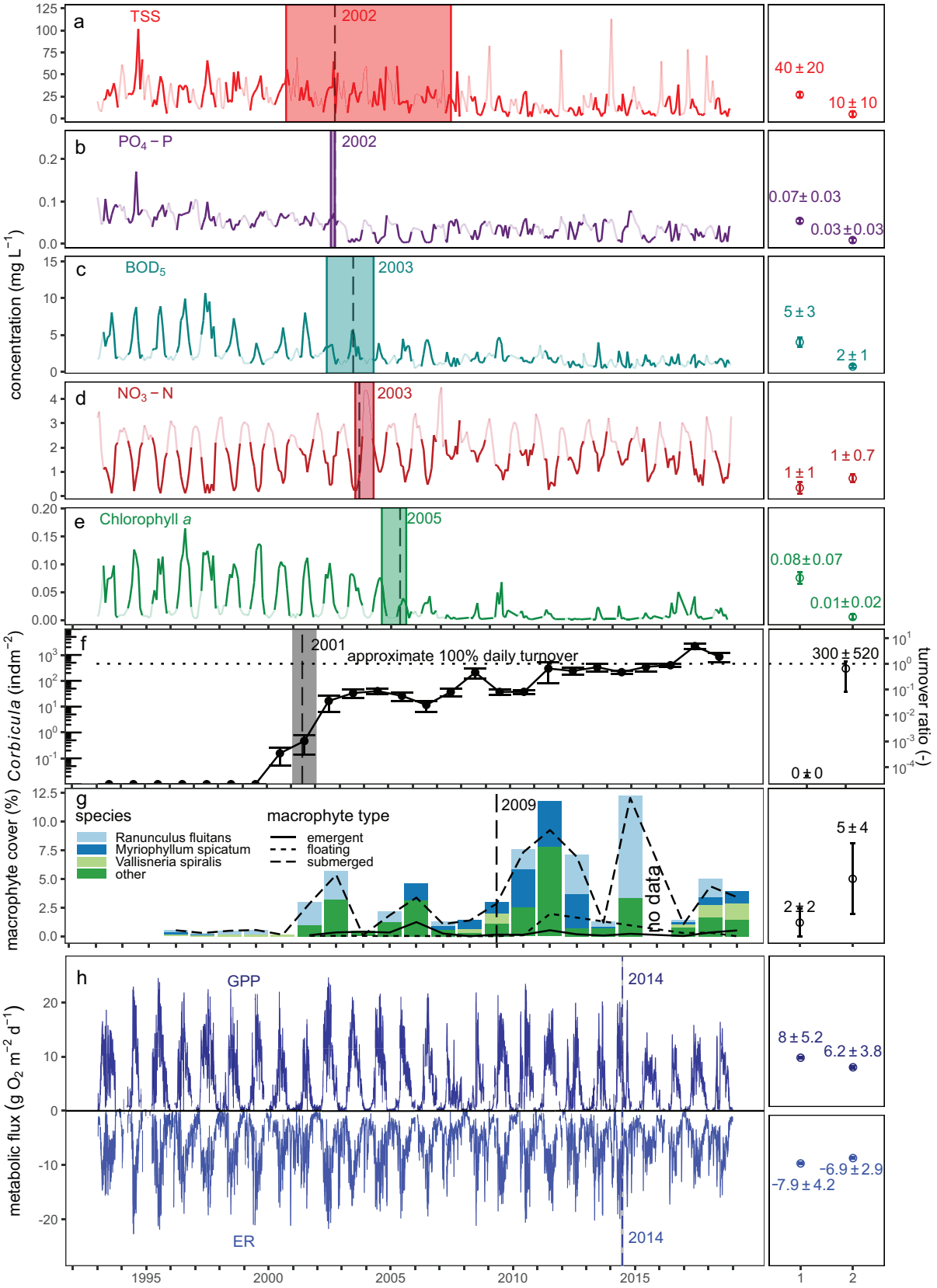
a
TSS
2002
40 ± 20
10 ± 10
b
PO4 – P
2002
0.07± 0.03
0.03 ±0.03
c
BOD5
2003
5 ± 3
2 ± 1
d
NO3 – N
2003
1 ± 1
1 ± 0.7
e
Chlorophyll a
2005
0.08±0.07
0.01±0.02
concentration (mg L−1)
f
2001
approximate 100% daily turnover
300 ± 520
0 ± 0
Corbicula (indm−2)
turnover ratio (-)
g
species
Ranunculus fluitans
Myriophyllum spicatum
Vallisneria spiralis
other
macrophyte type
emergent
floating
submerged
2009
no data
5 ± 4
2 ± 2
macrophyte cover (%)
h
GPP
2014
8 ± 5.2
6.2 ± 3.8
ER
2014
-6.9 ± 2.9
-7.9 ± 4.2
metabolic flux (g O2 m−2 d−1)
1995
2000
2005
2010
2015
1
2

communities expanded rapidly and coincidentally with water chemistry changes, exhibiting a detectable change point by 2009 (Fig. 1g). Estimated change points were robust to our priors and also to the inclusion or exclusion of variance in the model prescription.

These dramatic state variable shifts occurred contemporaneously with colonization of the middle Loire River by the invasive *Corbicula fluminea* clam (Fig. 1f). We detected a change point early in the time series of *Corbicula fluminea* densities in 2001, and by 2003 clam densities were sufficient to filter approximately 10% of the middle Loire River volume each day (i.e., turnover ratio = 0.1); by 2012 this had risen to approximately 100% (Fig. 1f, right panel values indicate the turnover ratio). State changes in summer PO_4–P, TSS, and chlorophyll *a* concentrations were approximately coincident with the initial increase in clam density (Fig. 1a–e), even though the filtration efficiency at the time of the state change remained relatively low.

Change points for GPP and ER were coincident in 2014, but clearly lagged the state variables by a decade or more, and credible intervals for metabolic change points were much smaller than for state variables. Changes in metabolic flux magnitudes before and after the change point were minor in comparison to state variables, with declines in mean daily GPP by only 25% and ER by 14%, respectively. The GPP decline was smaller still (near 10%) when indexed by summer low-flow duration, a strong indicator of metabolic pattern and magnitude (Fig. S6).

Phase space plots of the driver and response state variables (Fig. 2) further illustrate the rapidity of the ecosystem state shift, and stability of the pre- and postshift states. In particular, the clear bimodal clustering to the PO_4–P vs. chlorophyll (Fig. 2a) and PO_4–P vs. TSS (Fig. 2b) relationships are similar to the dynamics in shallow lakes exhibiting alternative stable states between algal dominance and macrophyte dominance (Scheffer et al. 2001). This clustering, especially for the relationship between PO_4-P and chlorophyll *a*, implies that both variables shifted around the same time. This limited evidence of hysteresis suggests that while the two states (phytoplankton and macrophyte dominance) are distinct and durable, the region of bistability (i.e., where both states are stable at the same levels of P loading) is narrow. Furthermore, the observed patterns between *Corbicula* and chlorophyll *a* (Fig. 2c) or PO_4–P (Fig. 2d) suggest a surprisingly monotonic transition. We also note the absence of any clear change in mean summer GPP (Fig. 2e–f), despite marked changes in both PO_4-P and chlorophyll *a*. This is consistent with our analyses in Fig. 1, suggesting modest changes in the metabolic regime that substantially lag the ecosystem state shift.

Shifts in ecosystem processes accompany a shifting metabolic regime

Abiotic controls on GPP weaken under macrophyte dominance

A best subsets multiple regression model explained ~70% of the variation in daily GPP ($F_{6,181} = 68.14$, $p < 0.001$). Discharge and median daily open sky irradiance were retained in every iteration of the exhaustive selection algorithm, suggesting their consistent role as dominant environmental drivers. In the final six-variable model, temperature, chlorophyll *a*, median daily open sky irradiance, discharge, TSS and DOC were all retained, but nutrient concentrations were not (Table S3). Temperature and chlorophyll *a* had the largest overall effect on GPP, whereas irradiance had an effect approximately half as large; all three effects were positive. Discharge had the greatest negative scaled model coefficient, followed by TSS, DOC, likely indicating their important role for water column light attenuation.

Due to the consistent dominant effects of light and discharge on GPP from the previous best subsets regression, we focused on how these abiotic controls changed from the plankton to macrophyte metabolic regimes. Overall scaled model coefficients suggest comparable, but opposing influence of discharge ($\beta = -2.81$) and light ($\beta = 2.00$) on growing season GPP ($F_{5;394} = 42.12$, $R_{adj}^2 = 0.34$, $p < 0.001$; Table S4). From the phytoplankton-dominated to macrophyte-dominated regimes, the negative influence of increasing discharge and the positive effects of increasing PAR declined by 50% (from −2.81 to −1.62) and 43% (from 2.00 to 0.99), respectively (Fig. 3a and Table S4).

Divergence of biological removal efficiencies for C and N

Removal efficiency for C increased with macrophtye dominance, but decreased for N (Fig. 3b). Over the 25-yr period, the log-linear rate of Da change for C was 0.03 yr^{-1} ($R^2 = 0.16$, $p = 0.04$), and for N was −0.17 yr^{-1} ($R^2 = 0.53$, $p < 0.001$; although the rate up to the 2005 state variable change point was 50% greater = 0.24 yr^{-1}). We note that if the entire summer period was analyzed, as opposed to only focusing on August, these log-linear rates are similar ($C = 0.03\ yr^{-1}$, $R^2 = 0.41$, $p < 0.001$; $N = -0.10\ yr^{-1}$, $R^2 = 0.46$, $p < .001$), confirming that the approach holds

Fig 1. Change points in ecosystem state and metabolism. Time series of ecosystem state variables (left panels)—including (**a**–**d**) water chemistry, (**e**) water column chlorophyll *a* concentrations, (**f**) *Corbicula fluminea* and (**g**) macrophyte density—as well as (**h**) open-channel metabolism (GPP and ER) in the middle Loire River for 1993–2018. Estimated change points (dashed lines) with 95% credible interval (shaded rectangles; credible intervals for metabolism are too narrow to see) are shown for each variable with text displaying the year of the change point. Dark line segments indicate growing season (April–October) observations while light segments are dormant season observations. Panels at right contrast the mean and 95% confidence intervals (mean ± SD in text) of each variable before (1) and after (2) the change point for that variable. Dotted line in panel (**f**) indicates a turnover ratio of 1 (turnover ratio values on right panel) for *Corbicula fluminea*; note log scale.

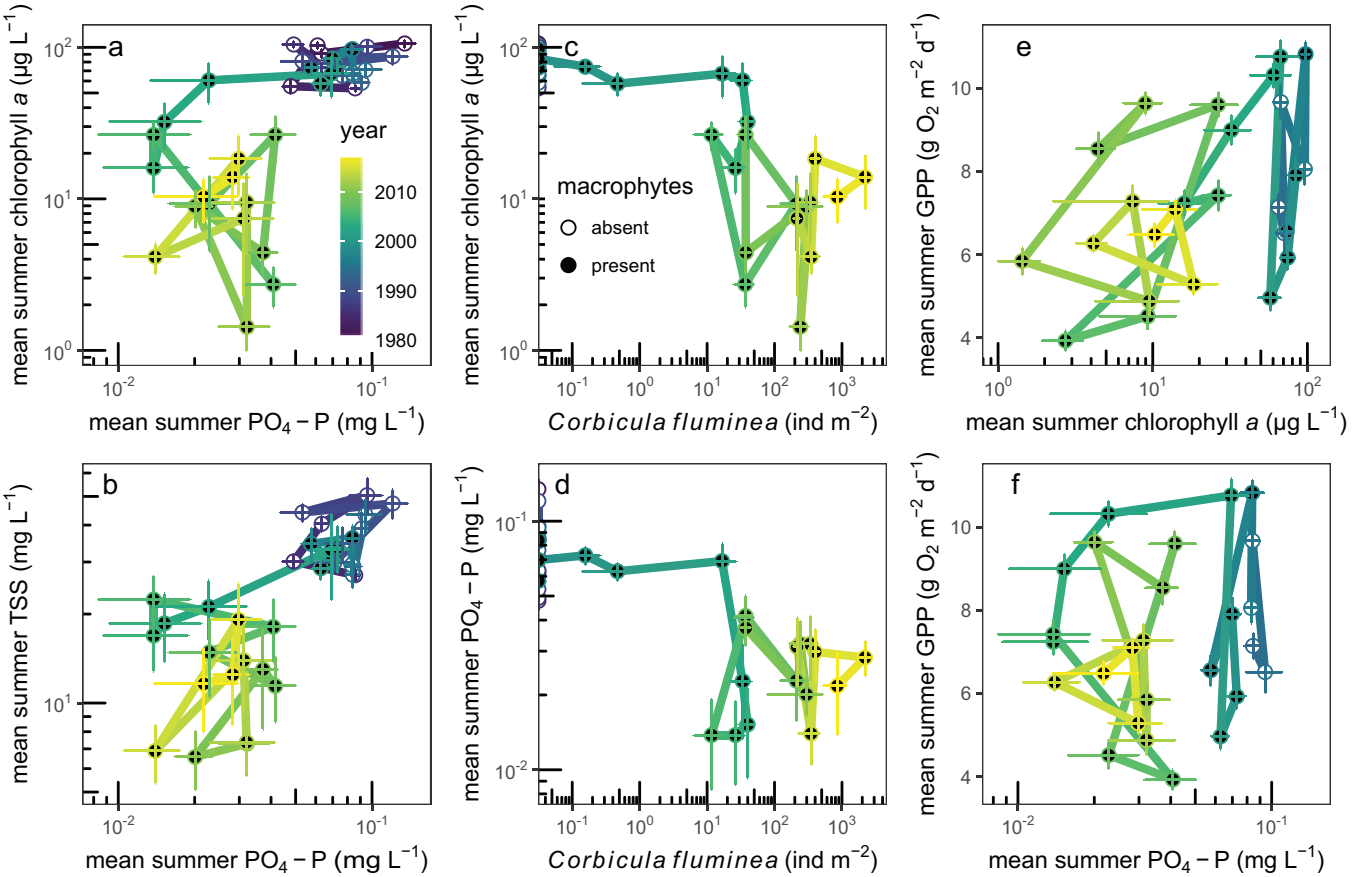

Fig 2. Phase space plots for middle Loire River variables. (**a**–**d**) Plots for predicted drivers (PO_4–P, *Corbicula fluminea* density) vs. response variables (chlorophyll *a* and TSS) colored by year with standard error bars and point type indicating presence of macrophytes; note log scales. The chlorophyll *a*- PO_4–P and the TSS- PO_4–P indicates two clusters of points, 1980–2004 (dark blue region) and 2005–2018 (green yellow region), suggesting two alternative states of water clarity/autotrophic community. In contrast, corbicula predictor plots do not exhibit as clear state separation, with more linear trends. (**e**–**f**) Plots for predicted drivers of GPP, with no indication of alternative stable metabolic regimes.

despite some uncertainty about variable benthic area due to variable discharge. Because the magnitude of ER was largely unchanged during this period, reduced particulate C flux due to declining phytoplankton concentrations in the river reach explains the 105% ± 12% increase in C removal efficiency under macrophyte dominance (from Da = 0.11 ± 0.03 to 0.22 ± 0.12; Fig. 3b). In contrast, NO_3–N biotic uptake efficiency decreased approximately 95% ± 24% (from Da = 1.50 ± 0.24 to 0.07 ± 0.06; Fig. 3b) due to both a combination of higher C:N ratios for primary producers lowering N demand and increased TIN concentrations (Fig. 1d). Notably, changes in C and N processing were not linear, with some evidence for regime shift behavior.

Shift from net autotrophy to net heterotrophy under macrophyte dominance

Summer NEP shifted from positive (autotrophic) to negative (heterotrophic) after the shift to macrophyte dominance, with concomitant shifts from longitudinal net C accrual (25 Mg C km^{-1}) to net C evasion (−25 Mg C km^{-1}; Fig. 3c). The NEP change point from autotrophy to heterotrophy aligns with the estimated change points for GPP and ER (blue vertical bars in Fig. 3), suggesting a relatively rapid, but delayed shift relative to ecosystem state changes.

Temporal decoupling of GPP and ER under macrophyte dominance

Up to the change point detected for ecosystem metabolism in 2014, *p*-values for Wald tests of Granger causality between GPP and ER were less than 0.05, indicating tight temporal coupling (Fig. 3d). This held for the entire prechange point time series except 2007, which was an unusually wet summer (Fig. S1). However, near the metabolic regime change point, and certainly after it, *p*-values were consistently greater than 0.05, indicating failure to reject the Granger causality null hypothesis, and implying temporal decoupling between GPP and ER at short time scales (<2 d).

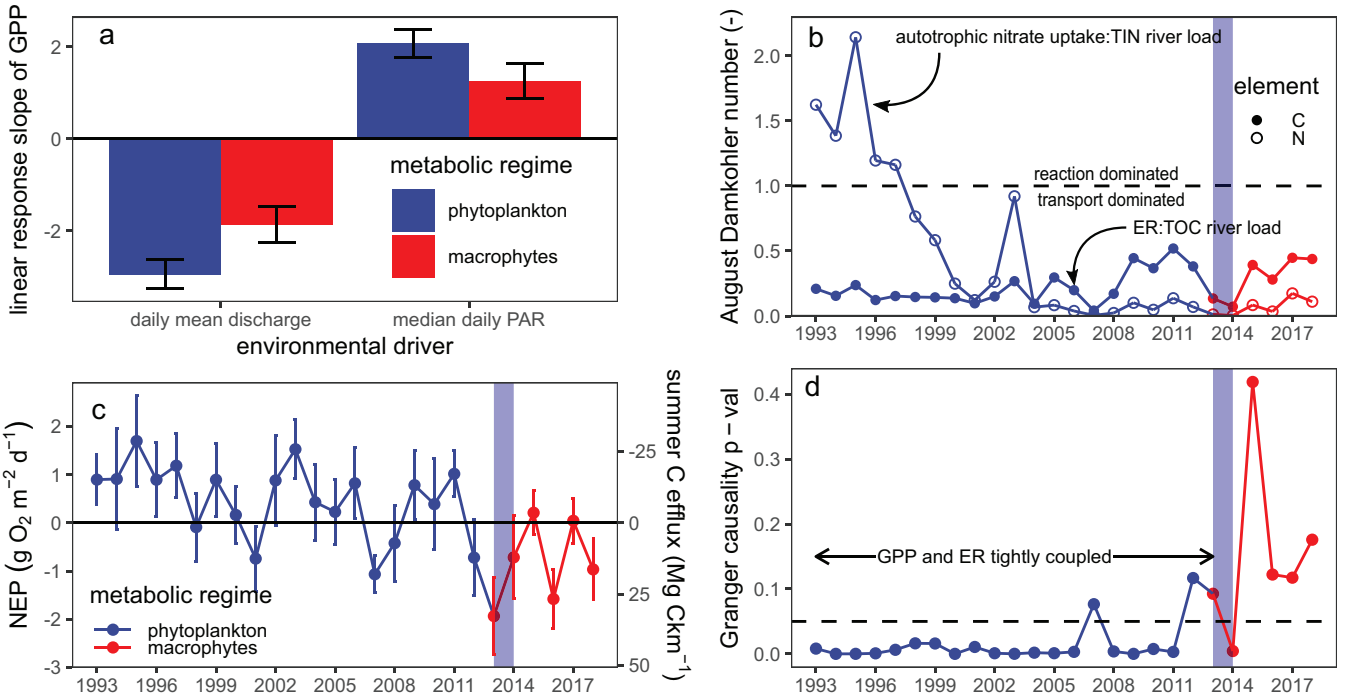

Fig 3. Features of a metabolic regime shift. The shift detected in GPP and ER in 2014 altered key features of the metabolic regime; for all panels, preshift measurements are shown in blue, with postshift measurements in red; vertical blue bars in (**b**–**d**) indicate estimated year of metabolic regime shift. (**a**) GPP became less sensitive to variability in discharge and light; bar heights indicate value of a scaled multiple regression model coefficient with metabolic regime as an interaction term and error bars indicate standard errors of the model coefficient. (**b**) River element cycling efficiency (Damköhler number, Da, which is the ratio of biological load removal to river load) was changed, with higher C processing efficiency (105% increase) due primarily to declining C loads, and lower N processing efficiency (95% reduction) due to reduced water column nitrate uptake by the dominant autotrophs. (**c**) The river shifted from autotrophic (mean summer NEP > 0) to heterotrophic (mean summer NEP < 0), leading to increased summer C efflux to the atmosphere. (**d**) Granger causality between GPP and ER, and between GPP and chlorophyll *a*, were no longer statistically significant (dashed line indicates $p = 0.05$) after the shift, indicating reduced temporal coupling between GPP and ER and GPP and chlorophyll *a* as macrophytes become dominant.

Ecosystem state regime shift predicted by early warning indicators for NEP

Typical state variable early warning indicators such as autocorrelation (i.e., ar[1], standard deviation, and skewness) did not unambiguously change in the years leading up to the detected ecosystem state shifts in 2002–2005 (Fig. S7), and the resulting Kendall τ values that indicate the robustness of early warning detection were highly variable and generally below the 0.5 threshold adopted to select viable indicators (Fig. S8). Moreover, indicators derived from these state variables time series were strikingly sensitive to rolling window size (2.5–12.5 yr) and detrending method (i.e., Gaussian, first differencing), limiting their utility in any forward-looking applications (Figs. S7, S8). While unstable early warning indication may be due to low observation frequency or strong dependence on discharge, we note that early warning indicators using hourly DO time series (i.e., DO daily maxima, minima, amplitude) were similarly sensitive to analysis decisions, lowering our confidence in their utility (Figs. S9, S10).

In contrast, time series statistics of NEP (ar[1], standard deviation, and skewness) were surprisingly informative for early warning detection of both the state shift and the metabolic regime shift (Fig. 4). These results were robust to detrending, likely because NEP in the Loire River has the desirable time series properties of stationarity ($t_{ADF} = -12$, $p < 0.01$) and normally distributed observations. Sensitivity analyses (Fig. S12) identified an optimal moving window length of 4 yr (16% of the dataset for metabolism fluxes). This window size provided the clearest signals, while still preserving a large amount of the pre- and postchange point dataset for analysis. We note that overall results for NEP were robust to smaller window sizes, down to 10% of each dataset. We observed increases in NEP standard deviation (Kendall $\tau = 0.56$) and ar(1) (Kendall $\tau = 0.6$) leading up to the state shift (Fig. 4b,c). The magnitude of skewness peaked in 2001 (Fig. 4d). NEP standard deviation, skewness, and ar(1) also increased prior to the metabolic change point in 2014 yielding what appears to be robust early warning for this functional shift.

Model concordance with NEP early warning indicators

Given the potential for NEP to provide reliable early warning indication of the state transition, we focused our model comparison on the time series patterns for NEP (Fig. 4e). For

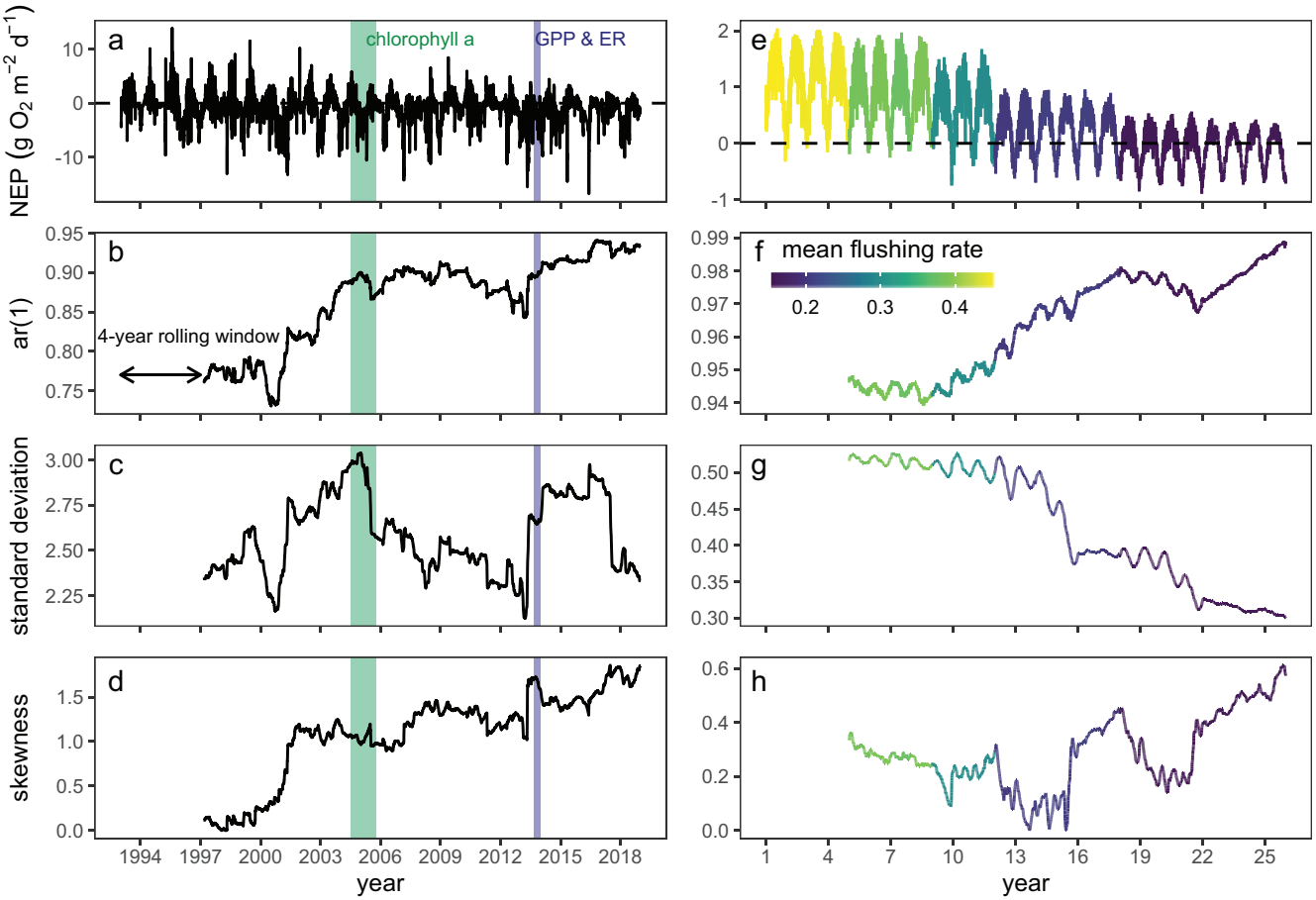

Fig 4. Early warning indicators for NEP time series derived from empirical assessment (**a**–**d**) compared to results from a simple river re-oligotrophic model (**e**–**h**). Shifts in ecosystem state (green bars) and metabolic regime (blue bars) are presaged by rolling window early warning indicators from (**a**) NEP time series. Candidate early warning indicators computed over a 4-yr moving window were (**b**) NEP autocorrelation with a 1-d lag, (**c**) standard deviation, and (**d**) skewness. Early warning indicators (rolling window = 4 yr) from 25 yr of (**e**) NEP output from a simple river re-oligotrophication mode. (**f**) Modeled ar(1) aligns with measurements, but (**g**) standard decreases throughout the entire model run as opposed to measurements, and (**h**) skewness exhibits an analogous increase to measurements.

the three early warning indicators we considered, there was strong correspondence between the empirical and modeled patterns. Although the absolute values differ significantly, early warning indicator trends in modeled ar(1) (Fig. 4f), standard deviation (Fig. 4g), and skewness (Fig. 4h) align with measured patterns, most strongly for ar(1), which increases as the state transition approaches. In contrast, standard deviation declined throughout the model run, analogous to measurements between state and metabolic regime change points. Skewness exhibited similar increasing behavior jump (near year 16) relative to measured values (near year 2001), despite not temporally aligning.

Discussion

The metabolic regime shift is damped and lagged compared to the ecosystem state shift

The temporal synchrony of change points among key variables provides strong support for an ecosystem state shift in the middle Loire River (Minaudo et al. 2015, 2020). Based on state variables, our observations situate the discrete shift in autotroph community from a water column, planktonic state to a sessile, benthic one around 2005. Macrophytes and associated epiphytic taxa ultimately replaced phytoplankton as dominant primary producers in the river. The predominance of submerged macrophytes (as opposed to floating or emergent taxa) aligns with expectations for re-oligotrophication (Hilton et al. 2006), with at least one pervasive species (*Myriophyllum spicatum*) known to exhibit phytoplankton allelopathy (Švanys et al. 2014).

Dramatic reductions in chlorophyll *a* and TSS are consistent with shifts reported elsewhere with advancing *Corbicula fluminea* invasions (Cohen et al. 1984; Pigneur et al. 2014), suggesting that these filter feeders are likely complicit with the sudden changes observed in the Loire (Minaudo et al. 2015). We note, however, phase space plots of chlorophyll *a* vs. PO_4–P imply a state shift more convincingly driven by internal nutrient or turbidity feedbacks than clam filtration (Fig. 2).

Our estimates of small turnover ratios (~ 0.1; Fig. 1f) and detailed modeling of clam filtration rates (Descy et al. 2012) further challenge the singular role of top-down control of the state transition by *Corbicula fluminea*, showing that densities (ca. 50 ind m^{-2}) at the time of the change points (2002–2005) were too low to drive the decline in phytoplankton biomass. Hence, while clam filtering is an important aspect of ecosystem change, it cannot, by itself, explain the rapid regime shift. We conclude that the state shift in the Loire River was likely induced via both bottom up (nutrient) and top down (clam) controls. Regardless of the relative importance of these controls, the change that was observed was rapid, coherent across variables, and durable in time.

Contrary to our expectations, the metabolic regime shift in the Middle Loire was not coincident with the observed shift associated with state transition from phytoplankton to macrophyte dominance. Moreover, the observed change in metabolic rates was small in comparison to the magnitude of state change and lagged the change points in chlorophyll *a* and PO_4–P by a decade (Fig. 1h). This suggests that decline in mean daily GPP (−25%) and ER (−14%) was decoupled in time and magnitude from regime shifts in the primary autotrophs (Fig. 1). These findings align with similar results from lake ecosystems (Zimmer et al. 2016)—perhaps due to relatively long hydraulic residence times in the middle Loire River that allow for internal feedbacks analogous to those from such shallow lake systems to develop. While shallow lake ecosystems have hydraulic residence times orders of magnitude greater than the middle Loire (e.g., 1 yr compared to 1 d), their magnitudes of C turnover times are often matched (e.g., 1 yr, Zimmer et al. 2016). We also observe a matching of hydraulic and C residence times (TOC:ER) in the middle Loire (~0.3 d), potentially suggesting that when these align, internal, biotically driven feedbacks can form and persist.

Critically, however, ecosystem state variables *did* exhibit a substantial threshold response, with clear indication of a regime shift to a new state (Fig. 2; Scheffer et al. 2001). The presence of a change point in the metabolism time series (Fig. 1h) along with the absence of evidence for alternative metabolic regimes (Fig. 2e–f) supports the idea that ecosystem function responses may be more gradual than (or even decoupled from) state responses to changing magnitudes of environmental drivers (Capon et al. 2015; Hillebrand et al. 2020). The maintenance of whole-system productivity despite order-of-magnitude declines in water column PO_4–P, TSS, and chlorophyll *a*, supports the general principle that energy inputs and disturbance, not nutrient concentrations, control river GPP (Jarvie et al. 2013; Bernhardt et al. 2018), consistent with revised models of river eutrophication (Hilton et al. 2006; O'Hare et al. 2018).

The decade lag between the shift in dominant autotrophs and the more modest metabolic regime shift could have several explanations. First, the timing of the shift to a macrophyte state may have been spatially heterogeneous in the study reach; our observations of macrophyte density are highly localized and at the lower end of the reach, which may reflect early changes in reach-scale shifts. Spatial patterns of macrophyte advancement, detectable from satellite imagery or detailed river surveys, may yield further insights into the potential patchiness of state transitions (Dakos et al. 2011). Second, P limitation to macrophyte GPP may lag their initial growth as they deplete the standing stock of sediment P on which they depend to overcome the declining upstream supply. Third, epiphyte density, which was not measured, but likely exerts nutrient and light control on macrophyte growth, may have increased over time, gradually reducing macrophyte GPP. Finally, the decline in GPP around 2015 (Fig. 1h) may arise from reduced summer flood incidence (Fig. S1a), allowing emergent (as opposed to submerged) macrophyte biomass to increase. This would lead to the underestimation of total river GPP as emergent plants exchange DO directly with the atmosphere, potentially creating an artificial change point due to underrepresented GPP fluxes.

Features of the metabolic regime shift

We observed clear evidence of altered biogeochemical processing related to shifts in ecosystem state and metabolic regime (Fig. 3). First, GPP became less sensitive to variability in the dominant environmental controls of light and discharge under macrophyte dominance (Fig. 3a). We attribute this weakened response to analogous shallow lake behavior wherein phytoplankton respond strongly to incident light due to rapid water column attenuation from self-shading, while clear water and phototropism under macrophyte dominance reduces this effect (de Tezanos Pinto and O'Farrell 2014).

Our observations support a substantial change in the relative processing efficiency of C and N in the river reach (Fig. 3b). The significant increase in removal efficiency for C (Fig. 3b) is almost entirely due to the reduced POC load (Minaudo et al. 2016) under clear water, macrophyte-dominated conditions. Indeed, the decrease in ER, which alone would reduce processing efficiency, highlights the overriding role of POC in raising reach-scale C removal efficiency. In contrast, the relative processing efficiency for N decreased markedly, and the reach shifted from a reaction- to a transport-dominated system (Fig. 3b). We attribute this to two primary factors: (1) higher C:N tissue stoichiometry in macrophytes compared to phytoplankton (Dickman et al. 2006; Xing et al. 2013), and (2) to increased N excretion from *Corbicula fluminea* clams (Lauritsen and Mozley 1989). Indeed, the onset of elevated summer NO_3–N concentrations (Figs. 1d, S4) under macrophyte dominance is plausibly attributed in part to decrease in NO_3–N uptake efficiency, noting that TN concentrations remained relatively constant (Fig. S13). These contrasting patterns for C and N removal efficiency lead to a generalized conceptual model for lotic re-oligotrophication driven by a shift in autotrophic community (Fig. 5).

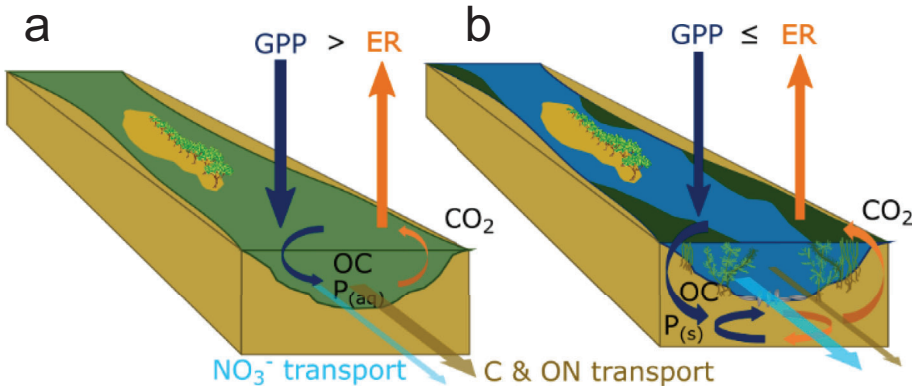

Fig 5. Conceptual model of a lotic ecosystem regime shift. (**a**) in a phytoplankton-dominated state, reach-scale GPP exceeds ER because fixed organic carbon (OC) in the water column is more easily flushed downstream; phosphorus ($P_{[aq]}$) is rapidly cycled between phytoplankton biomass and the water column; and high phytoplankton NO_3^- uptake leads to most N being bound in organic matter (ON). (**b**) In a rooted macrophyte-dominated state, OC production is primarily benthic, reducing downstream transport, and decreasing spatiotemporal coupling between GPP and ER; P associated with phytoplankton and water column heterotrophs is filtered by *Corbicula* and stored primarily in the benthos ($P_{[s]}$), whereas reduced water column uptake of NO_3^- leads to increased downstream NO_3^- fluxes.

Given persistent but unequal changes in ER and GPP with the transition to macrophyte dominance, NEP shifted from positive to negative in the middle Loire River (Figs. 3b, 5). This contrasts strikingly with the observed increase in riverine NEP during re-oligotrophication following improved wastewater treatment in the Oria River, Spain (Arroita et al. 2019). This is likely due to differences in how metabolism shifted between the two systems, with improved wastewater treatment primarily reducing ER (via effects on BOD_5) in the Oria River contrasted with principally autotrophic community shifts in the Loire that primarily impact GPP. It follows that each re-oligotrophication process likely depends on the primary mechanisms of change, and any generality across rivers will require conditioning our expectations based on primary modes of ecosystem change.

Finally, the Granger causality analysis supported our prediction of declining temporal coupling between GPP and ER in phytoplankton vs. macrophyte states (Figs. 3d, 5). Because ER includes AR, GPP implicitly influences that day's ER (Hall and Beaulieu 2013; Hotchkiss and Hall 2015). However, the influence of GPP on HR (HR = ER – AR) depends on the magnitude of allochthonous inputs, as well as quantity, quality and distribution of internal organic matter stocks (del Giorgio and Williams 2005). Allochthonous inputs typically dominate in small streams (Vannote et al. 1980), where GPP < < ER due to shading, and in streams with large exogenous loads (e.g., wastewater loads as in Arroita et al. (2019)). In larger rivers, autochthonous sources often dominate, but vary with contrasting autotroph communities. When phytoplankton dominate biomass production, net primary production (NPP = GPP – AR) is highly bioavailable and rapidly consumed by heterotrophic components of seston (Lair and Reyes-Marchant 1997; Hall and Beaulieu 2013), coupling HR to GPP over short time scales (Fig. 5a). Perhaps more importantly, plankton biomass is subject to downstream transport (i.e., "flushing"), especially during storms (Vilmin et al. 2016), limiting storage and thus reducing the capacity to sustain HR when GPP declines. In contrast, when rooted macrophytes are dominant, fixed C is less susceptible to flushing in addition to being less bioavailable (Fig. 5b). When biomass and organic matter can accumulate (including heterotrophic biomass like *Corbicula* sp.), HR can be sustained even as GPP varies in the short term, or declines over longer periods. This incrementally decouples HR from GPP, and this decouples ER (AR + HR) from GPP. Importantly, this behavior appears to be reversed in lakes where coupling between GPP and ER is higher in oligotrophic than eutrophic lakes, and where C excess may evade immediate respiration, leading to burial or export (Brothers et al. 2013).

Early warning indicators of the ecosystem state shift and metabolic regime shift

Early warning indicators of ecosystem regime shifts (Carpenter et al. 2011) derived from state variable time series in the middle Loire River were generally inconsistent with theoretical (Dakos et al. 2012) and experimental expectations (Scheffer et al. 2015). Moreover, these indicators based on state variable time series were highly sensitive to arbitrary choices for rolling window size or detrending method (e.g., Gaussian, first differencing), limiting their utility in forward-looking applications (Figs. S7, S8). While unstable early warning indication may be due to low observation frequency or strong dependence on discharge, we note that early warning indicators using hourly DO time series (i.e., DO daily maxima, minima, amplitude), which all yielded limited actionable insights, were similarly sensitive to analysis decisions, lowering our confidence in their utility (Figs. S9, S10).

In contrast, early warning indicators based on NEP were robust and informative (Figs. 4a–d, S11–S12), supporting our

hypothesis that the temporal dynamics of NEP yields a rich reservoir of information about ecosystem state and metabolic regime shifts. The indicators were well-behaved according to theoretical predictions (Dakos et al. 2012; Gsell et al. 2016). Specifically, magnitudes of ar(1), standard deviation, and skewness (interpreted as the growing influence of an alternative stable equilibrium near a tipping point; Guttal and Jayaprakash 2008) of NEP increased relatively monotonically up to the state shift. While the generality of using NEP as an early warning indicator for river state shifts is unclear, it is apparent that state shifts in lakes do not yield the same NEP patterns (Batt et al. 2013). Still, we note that both temporal and spatial uncertainties in metabolism estimates are lower in rivers due to advection and turbulent mixing. We posit that when metabolic estimates are reasonably well constrained, as they are in long riverine time series like this one on the Loire River, NEP yields a useful, integrative, and predictive measure of ecosystem state and function, similar to patterns predicted between forest productivity and ecosystem regime shifts (Boulton et al. 2013). With the emergence of long time DO series in many rivers (Appling et al. 2018), the utility and generality of NEP shifts as metrics or even forecasts of ecosystem change will be increasingly testable.

Contrasting patterns of net ecosystem productivity between lotic system states

Decoupling between GPP and ER is difficult to discern from their correlation alone (Sugihara et al. 2012), but is readily detected from the time series properties of their sum (NEP). While individual time series of GPP and ER are inherently autocorrelated because of the temporal dynamics of their shared drivers (i.e., solar radiation and temperature) and biomass dependence, the degree to which they exhibit *the same* autocorrelation depends on their temporal coupling, with stronger coupling yielding more similar autocorrelation structures. NEP is the sum of two signals, so its autocorrelation ($R_{\mathrm{NEP,NEP}}$) is mathematically defined as:

$$R_{\mathrm{NEP,NEP}} = (R_{\mathrm{GPP,GPP}} + R_{\mathrm{ER,ER}}) + (R_{\mathrm{GPP,ER}} + R_{\mathrm{ER,GPP}})$$

where $R_{x,y}$ is the correlation matrix of vectors x and y. Because ER and GPP have opposite signs, their cross correlations (right hand parentheses) are negative. As the processes decouple, their cross-correlation declines, and NEP autocorrelation increases, yielding an integrative measure of the underlying structure of riverine metabolic regimes. This axiomatic result is also intuitive. Stronger ecosystem memory in the form of stored biomass should increase NEP stability. Our simple river reach growth model, with a single free parameter to describe biomass flushing yields the same conclusion (Fig. 4e–h). That model recreates the metabolic dynamics of the shift from phytoplankton to macrophytes, including gradual NEP declines, and shifting autocorrelation and skewness patterns that provide early indication of ecosystem state changes.

Implications for lotic system management

An abrupt and durable state shift in this large, low-gradient river implies plausible evidence of internal feedbacks that were previously thought to be minimal in lotic ecosystems (Hilton et al. 2006; Hilt 2015), with important implications for management. We note that these feedbacks do appear to be weaker than in lentic systems, as indicated by the short lag between changes in top-down (*Corbicula fluminea*) or bottom-up (PO_4–P) controls and the shift from phytoplankton to macrophytes, which may also suggest socially palatable recovery timeframes. The surprisingly weak coupling between ecosystem state and metabolic rates, often attributed to community compensation (Vis et al. 2007; Zimmer et al. 2016), further implies that metabolism per se may not always be useful for evaluating river ecosystem recovery (sensu Palmer and Ruhi 2019), especially when reduction in phytoplankton blooms is the target. Perhaps in shallow lotic systems where nutrients are plentiful from upstream resupply (Covino et al. 2018), ecosystem metabolic rates organize to maximize power output (Odum and Pinkerton 1955), and thus reflect light availability regardless of community structure (Morgan Ernest and Brown 2001). Critically, however, the temporal patterns and coupling of GPP and ER signals *do* change, with dynamics that successfully predict both riverine state shifts and metabolic regime shifts, and which exert measurable impacts on biogeochemical processing efficiency.

State changes are important management considerations for rivers worldwide, highlighting the urgency of understanding linked changes in the regulation and provisioning of key river functions. With the joint challenges of changing human management and changing climate, measurements that reveal the timing and magnitude of ecosystem responses and provide early warnings of riverine state shifts are of obvious utility. We suggest that monitoring the metabolic regimes of rivers, and specifically tracking NEP, may yield early warning indication of state shifts, and thus provide useful interim targets for management toward river re-oligotrophication goals. While the observation that autotrophic state and primary production are surprisingly decoupled in the Loire River invites refinements of eutrophication conceptual models in lotic vs. lentic waters, the metabolic response is, nonetheless, highly informative about the dynamics of state shifts. Long time series of river metabolism like those from the Loire River are invaluable for probing this link between ecosystem state and function, detecting their shifts, and documenting progress toward ecosystem restoration objectives.

References

Appling, A. P., R. O. Hall Jr., C. B. Yackulic, and M. Arroita. 2018. Overcoming equifinality: Leveraging long time series for stream metabolism estimation. J. Geophys. Res. Biogeo. **123**: 624–645.

Arroita, M., A. Elosegi, and R. O. Hall. 2019. Twenty years of daily metabolism show riverine recovery following sewage abatement: Long-term recovery of a polluted river. Limnol. Oceanogr. **64**: S77–S92. doi:10.1002/lno.11053

Baratelli, F., N. Flipo, and F. Moatar. 2016. Estimation of stream-aquifer exchanges at regional scale using a distributed model: Sensitivity to in-stream water level fluctuations, riverbed elevation and roughness. J. Hydrol. **542**: 686–703. doi:10.1016/j.jhydrol.2016.09.041

Batt, R. D., S. R. Carpenter, J. J. Cole, M. L. Pace, and R. A. Johnson. 2013. Changes in ecosystem resilience detected in automated measures of ecosystem metabolism during a whole-lake manipulation. Proc. Natl. Acad. Sci. **110**: 17398–17403.

Bernhardt, E. S., J. B. Heffernan, N. B. Grimm, and and others. 2018. The metabolic regimes of flowing waters. Limnol. Oceanogr. **63**: S99–S118.

Biggs, R., S.R. Carpenter, S. R., and W.A. Brock. 2009. Turning back from the brink: Detecting an impending regime shift in time to avert it. Proc. Natl. Acad. Sci., **106**, 826–831.

Boulton, C. A., P. Good, and T. M. Lenton. 2013. Early warning signals of simulated Amazon rainforest dieback. Theor Ecol **6**: 373–384. doi:10.1007/s12080-013-0191-7

Brothers, S. M., S. Hilt, K. Attermeyer, and and others. 2013. A regime shift from macrophyte to phytoplankton dominance enhances carbon burial in a shallow, eutrophic lake. Ecosphere **4**: 1–17.

Capon, S. J., A. J. J. Lynch, N. Bond, and and others. 2015. Regime shifts, thresholds and multiple stable states in freshwater ecosystems; a critical appraisal of the evidence. Sci. Total Environ. **534**: 122–130. doi:10.1016/j.scitotenv.2015.02.045

Carpenter, S. R., and W. A. Brock. 2006. Rising variance: A leading indicator of ecological transition. Ecol. Lett. **9**: 311–318.

Carpenter, S. R., J. J. Cole, M. L. Pace, and and others. 2011. Early warnings of regime shifts: A whole-ecosystem experiment. Science **332**: 1079–1082.

Cohen, R. R. H., P. V. Dresler, E. J. P. Phillips, and R. L. Cory. 1984. The effect of the Asiatic clam, *Corbicula fluminea*, on phytoplankton of the Potomac River, Maryland. Limnol. Oceanogr. **29**: 170–180. doi:10.4319/lo.1984.29.1.0170

Cohen, M. J., M. J. Kurz, J. B. Heffernan, J. B. Martin, R. L. Douglass, C. R. Foster, and R. G. Thomas. 2013. Diel phosphorus variation and the stoichiometry of ecosystem metabolism in a large spring-fed river. Ecological Monographs **83**: 155–176. doi:https://doi.org/10.1890/12-1497.1

Cole, J. J., Y. T. Prairie, N. F. Caraco, and and others. 2007. Plumbing the global carbon cycle: Integrating inland waters into the terrestrial carbon budget. Ecosystems **10**: 172–185.

Covino, T. P., E. S. Bernhardt, and J. B. Heffernan. 2018. Measuring and interpreting relationships between nutrient supply, demand, and limitation. Freshwater Science **37**: 448–455.

Dakos, V., S. Kéfi, M. Rietkerk, E. H. van Nes, and M. Scheffer. 2011. Slowing down in spatially patterned ecosystems at the brink of collapse. Am. Nat. **177**: E153–E166. doi:10.1086/659945

Dakos, V., S. R. Carpenter, W. A. Brock, and and others. 2012. Methods for detecting early warnings of critical transitions in time series illustrated using simulated ecological data. PloS one: **7**: e41010.

Descy, J.-P., M. Leitao, E. Everbecq, J. S. Smitz, and J.-F. Deliège. 2012. Phytoplankton of the river Loire, France: A biodiversity and modelling study. J. Plankton Res. **34**: 120–135. doi:10.1093/plankt/fbr085

Diamond, J. 2021. Middle Loire River hydrochemistry, biology, and metabolism data, HydroShare, http://www.hydroshare.org/resource/b1547a02846b4a88a8273aa229454eb0

Dickman, E. M., M. J. Vanni, and M. J. Horgan. 2006. Interactive effects of light and nutrients on phytoplankton stoichiometry. Oecologia **149**: 676–689. doi:10.1007/s00442-006-0473-5

Escoffier, N., N. Bensoussan, L. Vilmin, N. Flipo, V. Rocher, A. David, F. Métivier, and A. Groleau. 2018. Estimating ecosystem metabolism from continuous multi-sensor measurements in the Seine River. Environ. Sci. Pollut. Res. **25**: 23451–23467.

European Environmental Commission. 1991. Council directive 91/676/EEC of 12 December 1991 concerning the protection of waters against pollution caused by nitrates from agricultural sources. Commun: Off. J. Eur.

Floury, M., P. Usseglio-Polatera, M. Ferreol, C. Delattre, and Y. Souchon. 2013. Global climate change in large European rivers: Long-term effects on macroinvertebrate communities and potential local confounding factors. Glob. Chang. Biol. **19**: 1085–1099.

del Giorgio, P. A., and P. L. B. Williams. 2005. The global significance of respiration in aquatic ecosystems: From single cells to the biosphere, pp. 267–303. In P. A. Giorgio and P. L. B. Williams [eds.], Respiration in aquatic ecosystems. Oxford University Press, New York.

Gsell, A. S., and and others. 2016. Evaluating early-warning indicators of critical transitions in natural aquatic ecosystems. Proc. Natl. Acad. Sci. **113**: E8089–E8095.

Guttal, V., and C. Jayaprakash. 2008. Changing skewness: An early warning signal of regime shifts in ecosystems. Ecol. Lett. **11**: 450–460. doi:10.1111/j.1461-0248.2008.01160.x

Hall, R. O., and J. J. Beaulieu. 2013. Estimating autotrophic respiration in streams using daily metabolism data. Freshwater Science **32**: 507–516. doi:10.1899/12-147.1

Heffernan, J. B. 2008. Wetlands as an alternative stable state in desert streams. Ecology **89**: 1261–1271.

Heffernan, J. B., and M. J. Cohen. 2010. Direct and indirect coupling of primary production and diel nitrate dynamics in a subtropical spring-fed river. Limnol. Oceanogr. **55**: 677–688. doi:https://doi.org/10.4319/lo.2010.55.2.0677

Hillebrand, H., I. Donohue, W. S. Harpole, D. Hodapp, M. Kucera, A. M. Lewandowska, J. Merder, J. M. Montoya, and J. A. Freund. 2020. Thresholds for ecological responses to global change do not emerge from empirical data. Nature Ecology & Evolution **4**: 1502–1509.

Hilt, S., J. Köhler, H.-P. Kozerski, E. H. van Nes, and M. Scheffer. 2011. Abrupt regime shifts in space and time along rivers and connected lake systems. Oikos **120**: 766–775.

Hilt, S. 2015. Regime shifts between macrophytes and phytoplankton–concepts beyond shallow lakes, unravelling stabilizing mechanisms and practical consequences. Limnetica **34**: 467–480.

Hilt, S., S. Brothers, E. Jeppesen, A. J. Veraart, and S. Kosten. 2017. Translating regime shifts in Shallow Lakes into changes in ecosystem functions and services. Bioscience **67**: 928–936. doi:10.1093/biosci/bix106

Hilton, J., M. O'Hare, M. J. Bowes, and J. I. Jones. 2006. How green is my river? A new paradigm of eutrophication in rivers. Sci. Total Environ. **365**: 66–83.

Hotchkiss, E. R., and R. O. Hall. 2015. Whole-stream 13C tracer addition reveals distinct fates of newly fixed carbon. Ecology **96**: 403–416. doi:10.1890/14-0631.1

Ibáñez, C., C. Alcaraz, N. Caiola, and and others. 2012. Regime shift from phytoplankton to macrophyte dominance in a large river: Top-down versus bottom-up effects. Sci. Total Environ. **416**: 314–322.

Ibáñez, C., and J. Peñuelas. 2019. Changing nutrients, changing rivers. Science **365**: 637–638. doi:10.1126/science.aay2723

Jarvie, H. P., A. N. Sharpley, P. J. A. Withers, J. T. Scott, B. E. Haggard, and C. Neal. 2013. Phosphorus mitigation to Control River eutrophication: Murky waters, inconvenient truths, and "Postnormal" science. J. Environ. Qual. **42**: 295–304. doi:10.2134/jeq2012.0085

King, S. A., J. B. Heffernan, and M. J. Cohen. 2014. Nutrient flux, uptake, and autotrophic limitation in streams and rivers. Freshwater Science **33**: 85–98.

Koenig, L. E., A. M. Helton, P. Savoy, E. Bertuzzo, J. B. Heffernan, R. O. Hall Jr., and E. S. Bernhardt. 2019. Emergent productivity regimes of river networks. Limnology and Oceanography Letters **4**: 173–181.

Lair, N., and P. Reyes-Marchant. 1997. The potamoplankton of the middle Loire and the role of the "moving littoral" in downstream transfer of algae and rotifers. Hydrobiologia **356**: 33–52. doi:10.1023/A:1003127230386

Lauritsen, D. D., and S. C. Mozley. 1989. Nutrient excretion by the Asiatic clam *Corbicula fluminea*. Journal of the North American Benthological Society **8**: 134–139.

Lindeløv, J. 2020. Mcp: An R package for regression with multiple change points. doi:10.31219/osf.io/fzqxv

Lumley, T. 2020. Leaps: Regression subset selection. R package version 3.1. https://CRAN.R-project.org/package=leaps

McDowell, W. G., and J. E. Byers. 2019. High abundance of an invasive species gives it an outsized ecological role. Freshw. Biol. **64**: 577–586. doi:10.1111/fwb.13243

Minaudo, C., M. Meybeck, F. Moatar, N. Gassama, and F. Curie. 2015. Eutrophication mitigation in rivers: 30 years of trends in spatial and seasonal patterns of biogeochemistry of the Loire River (1980–2012). Biogeosciences **12**: 2549–2563.

Minaudo, C., F. Moatar, A. Coynel, H. Etcheber, N. Gassama, and F. Curie. 2016. Using recent high-frequency surveys to reconstitute 35 years of organic carbon variations in a eutrophic lowland river. Environ. Monit. Assess. **188**: 41.

Minaudo, C., A. Abonyi, M. Leitao, A. M. Lançon, M. Floury, J. P. Descy, and F. Moatar. 2020. Long-term impacts of nutrient control, climate change, and invasive clams on phytoplankton and cyanobacteria biomass in a large temperate river. Sci. Total Environ. **756**: 144074.

Moatar, F., J. Miquel, and A. Poirel. 2001. A quality-control method for physical and chemical monitoring data. Application to dissolved oxygen levels in the river Loire (France). J. Hydrol. **252**: 25–36. doi:10.1016/S0022-1694(01)00439-5

Moatar, F., and M. Meybeck. 2005. Compared performances of different algorithms for estimating annual nutrient loads discharged by the eutrophic River Loire. Hydrolog. Process. Int. J. **19**: 429–444.

Moatar, F., and J. Gailhard. 2006. Water temperature behaviour in the River Loire since 1976 and 1881. C. R. Geosci. **338**: 319–328.

Morgan Ernest, S. K., and J. H. Brown. 2001. Homeostasis and compensation: The role of species and resources in ecosystem stability. Ecology **82**: 2118–2132.

Moritz, S. and T. Bartz-Beielstein. 2017. imputeTS: Time series missing value imputation in R. R J., **9**: 207–218. doi:10.32614/RJ-2017-009.

Mulholland, P. J., C. S. Fellows, J. L. Tank, and and others. 2001. Inter-biome comparison of factors controlling stream metabolism. Freshw. Biol. **46**: 1503–1517. doi:10.1046/j.1365-2427.2001.00773.x

O'Connor, D. J., and W. E. Dobbins. 1958. Mechanism of reaeration in natural streams. Trans. Am. Soc. Civil Eng. **123**: 641–666.

Odum, H. T. 1956. Primary production in flowing waters 1. Limnol. Oceanogr. **1**: 102–117.

Odum, H. T., and R. C. Pinkerton. 1955. Time's speed regulator: The optimum efficiency for maximum power output in physical and biological systems. Am. Sci. **43**: 331–343.

O'Hare, M. T., A. Baattrup-Pedersen, I. Baumgarte, and and others. 2018. Responses of aquatic plants to eutrophication in rivers: A revised conceptual model. Front. Plant Sci. **9**: 451.

Palmer, M., and A. Ruhi. 2019. Linkages between flow regime, biota, and ecosystem processes: Implications for river restoration. Science **365**: eaaw2087.

Pigneur, L.-M., E. Falisse, K. Roland, E. Everbecq, J.-F. Deliège, J. S. Smitz, K. V. Doninck, and J.-P. Descy. 2014. Impact of invasive Asian clams, Corbicula spp., on a large river ecosystem. Freshw. Biol. **59**: 573–583. doi:10.1111/fwb.12286

Savoy, P., A. P. Appling, J. B. Heffernan, E. G. Stets, J. S. Read, J. W. Harvey, and E. S. Bernhardt. 2019. Metabolic rhythms in flowing waters: An approach for classifying river productivity regimes. Limnol. Oceanogr. **64**: 1835–1851.

Scheffer, M., S. Carpenter, J. A. Foley, C. Folke, and B. Walker. 2001. Catastrophic shifts in ecosystems. Nature **413**: 591–596. doi:10.1038/35098000

Scheffer, M., and E. Jeppesen. 2007. Regime shifts in Shallow Lakes. Ecosystems **10**: 1–3. doi:10.1007/s10021-006-9002-y

Scheffer, M., S. R. Carpenter, V. Dakos, and E. H. van Nes. 2015. Generic indicators of ecological resilience: Inferring the chance of a critical transition. Annu. Rev. Ecol. Evol. Syst. **46**: 145–167.

Seitzinger, S. P., R. V. Styles, E. W. Boyer, R. B. Alexander, G. Billen, R. W. Howarth, B. Mayer, and N. Van Breemen. 2002. Nitrogen retention in rivers: Model development and application to watersheds in the northeastern USA, p. 199–237.*In* The nitrogen cycle at regional to global scales. Springer.

Smith, V. H., G. D. Tilman, and J. C. Nekola. 1999. Eutrophication: Impacts of excess nutrient inputs on freshwater, marine, and terrestrial ecosystems. Environ. Pollut. **100**: 179–196. doi:10.1016/S0269-7491(99)00091-3

Sugihara, G., R. May, H. Ye, C. Hsieh, E. Deyle, M. Fogarty, and S. Munch. 2012. Detecting causality in complex ecosystems. Science **338**: 496–500. doi:10.1126/science.1227079

Švanys, A., R. Paškauskas, and S. Hilt. 2014. Effects of the allelopathically active macrophyte *Myriophyllum spicatum* on a natural phytoplankton community: A mesocosm study. Hydrobiologia **737**: 57–66.

de Tezanos Pinto, P., and I. O'Farrell. 2014. Regime shifts between free-floating plants and phytoplankton: A review. Hydrobiologia **740**: 13–24.

Vannote, R. L., G. W. Minshall, K. W. Cummins, J. R. Sedell, and C. E. Cushing. 1980. The river continuum concept. Can. J. Fish. Aquat. Sci. **37**: 130–137. doi:10.1139/f80-017

Ventura, M., L. Liboriussen, T. Lauridsen, M. Søndergaard, M. Søndergaard, and E. Jeppesen. 2008. Effects of increased temperature and nutrient enrichment on the stoichiometry of primary producers and consumers in temperate shallow lakes. Freshw. Biol. **53**: 1434–1452.

Vilmin, L., N. Flipo, N. Escoffier, V. Rocher, and A. Groleau. 2016. Carbon fate in a large temperate human-impacted river system: Focus on benthic dynamics. Global Biogeochem. Cycles **30**: 1086–1104. doi:10.1002/2015GB005271

Vis, C., C. Hudon, R. Carignan, and P. Gagnon. 2007. Spatial analysis of production by Macrophytes, phytoplankton and Epiphyton in a large river system under different water-level conditions. Ecosystems **10**: 293–310. doi:10.1007/s10021-007-9021-3

Williamson, C. E., W. Dodds, T. K. Kratz, and M. A. Palmer. 2008. Lakes and streams as sentinels of environmental change in terrestrial and atmospheric processes. Front. Ecol. Environ. **6**: 247–254. doi:10.1890/070140

Xing, W., H.-P. Wu, B.-B. Hao, and G.-H. Liu. 2013. Stoichiometric characteristics and responses of submerged macrophytes to eutrophication in lakes along the middle and lower reaches of the Yangtze River. Ecol. Eng. **54**: 16–21. doi:10.1016/j.ecoleng.2013.01.026

Zimmer, K. D., W. O. Hobbs, L. M. Domine, B. R. Herwig, M. A. Hanson, and J. B. Cotner. 2016. Uniform carbon fluxes in shallow lakes in alternative stable states. Limnol. Oceanogr. **61**: 330–340.

Acknowledgments

Jacob S. Diamond is supported by POI FEDER Loire n°2017-EX001784, Water Agency of Loire Catchment AELB, and Université de Tours, France. This work was also supported by the EUR H2O'Lyon, French ANR-17-EURE-0018 grant. The authors thank Gwenaël Abril (CNRS, BOREA, MNHN) for the floating dome measurements and Damien Hemeray (Réserve naturelle nationale de Saint-Mesmin Loiret Nature Environnement) for the macrophyte data. The authors also thank two anonymous reviewers and the editorial team for their thorough review and suggestions that improved this manuscript.

Conflict of Interest

None declared.

Submitted 30 July 2020
Revised 18 January 2021
Accepted 25 April 2021

Associate editor: James Heffernan